Quantitative Estimation of Exchange Interaction Energy Using Two-Electron Vertical Double Quantum Dots

T. Kodera,[1] K. Ono,[2] Y. Kitamura,[3] Y. Tokura,[4,5] Y. Arakawa,[1,6] and S. Tarucha[1,3,4]

[1]*Institute for Nano Quantum Information Electronics, the University of Tokyo, 4-6-1 Komaba, Meguro-ku, Tokyo 153-8505, Japan*
[2]*RIKEN, 2-1, Hirosawa, Wako-shi, Saitama 351-0198, Japan*
[3]*School of Engineering, the University of Tokyo, 7-3-1, Hongo, Bunkyo-ku, Tokyo 113-8656, Japan*
[4]*ICORP-JST, 3-1, Morinosato Wakamiya, Atsugi-shi, Kanagawa 243-0198, Japan*
[5]*NTT Basic Research Laboratories, 3-1, Morinosato Wakamiya, Atsugi-shi, Kanagawa 243-0198, Japan*
[6]*Institute of Industrial Science, Research Center for Advanced Science and Technology, the University of Tokyo, 4-6-1 Komaba, Meguro-ku, Tokyo, 153-8505, Japan**

(Received 26 January 2009; published 8 April 2009)

We use Pauli-spin blockade in two-electron vertical double quantum dots to quantitatively estimate the exchange energy J in a wide range of interdot level detuning Δ and fully compare it with calculations. Pauli-spin blockade is lifted via a singlet- (S-)triplet (T) transition mediated by hyperfine coupling, which abruptly occurs in our devices when the S-T transition energy or J is compensated by the Zeeman energy. We use this feature to derive J depending on Δ between the S-S and T-T resonances. The obtained J versus Δ including the resonance effect is perfectly reproduced by Hubbard model calculations.

DOI: 10.1103/PhysRevLett.102.146802 PACS numbers: 73.23.Hk, 73.63.Kv, 75.30.Et

Detecting and manipulating the exchange interaction between two electrons is at the heart of spin-based quantum information processing, especially for implementing quantum entanglement and a universal set of quantum gates [1,2]. Semiconductor double quantum dots (QDs) holding two electrons are relevant for this purpose, because the spin exchange energy J or energy separation between a singlet (S) state and a triplet (T) state can be varied both electrically and magnetically [3,4]. This method of J modulation has recently been used to prepare electron spin qubits and to control electron spin-nuclear spin coupling in a double QD [5–7]. Coherent manipulation of single electron spins or electron spin qubits has been realized by controlling J to swap electrons between the two QDs [8,9]. S-T mixing in a fluctuating nuclear field B_N has been explored by making J sufficiently smaller than the electron Zeeman energy E_N corresponding to B_N [10]. The dephasing time of two-electron spin states has been measured by controlling the ratio between J and E_N [11].

J depends strongly on the interdot level detuning Δ, and in all of the above described experiments the Δ-dependent J is a key parameter. Here J is simply defined as the spin excitation energy between S and T in a double QD. This J value usually decreases as Δ increases; however, this is not the case near interdot resonance, because the resonant states are hybridized to enhance the S-T separation [see Fig. 1(b)]. J vs Δ has been only partly examined by experiment and has never been well compared to theory [12]. In this Letter we use a vertically coupled double QD to derive J vs Δ in a wide range of Δ between two resonance points: S-S resonance ($\Delta = 0$) and T-T resonance ($\Delta = \Delta_T$) [Fig. 1(b)]. Note the threshold of PSB lifting is much better defined in vertical double QDs than in lateral double QDs. We find good agreement in J vs Δ between experiment and calculations.

To evaluate J, we use the hyperfine interaction mediated by lifting of the Pauli-spin blockade (PSB). PSB occurs

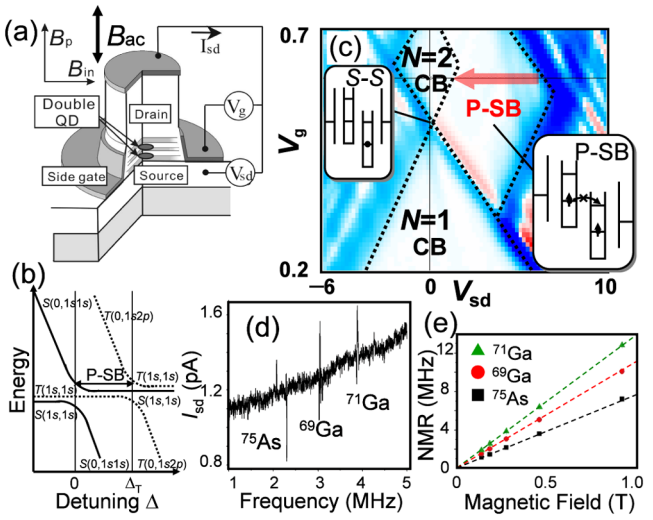

FIG. 1 (color online). (a) Schematic picture of the double QD and measurement setups. The static magnetic fields B_p and B_{in} are applied perpendicular and parallel to the QD plane. The ac magnetic field B_{ac} for NMR measurements is applied perpendicular to the QD plane. (b) Energy diagram for a two-electron ground state and the excited states with potential detuning Δ as a parameter. (c) Color-scale plot of dI_{sd}/dV_{sd} in the $V_{sd} - V_g$ plane measured for device A at 1.5 K. The white region corresponds to the blockade. The energy diagrams of PSB and S-S resonance are indicated. (d) I_{sd} as a function of the frequency of B_{ac} under an in-plane magnetic field of $B_{in} = 300$ mT. NMR signals for ^{75}As, ^{69}Ga, and ^{71}Ga are detected. (e) NMR signal positions as a function of B_{in} for the nuclei.

between $\Delta = 0$ and $\Delta = \Delta_T$ by setting up a T state over the two QDs as a long-lived excited state. It is lifted through a T to S transition by compensating for J with the electron Zeeman energy, E_Z. This S-T transition is signified as an abrupt increase of the leakage current in the PSB region at a certain magnetic field B_{sw} where $J = E_Z$ $(= g\mu_B B_{sw})$ [13]. Then, B_{sw} is a good measure for evaluating J. An error may arise in this derivation from dynamical nuclear polarization (DNP). The DNP effect is, however, negligible when the applied external magnetic field is small [5], which is the case for the present work.

In a vertical double QD, Δ is varied as a function of the bias voltage (V_{sd}) applied between the source and drain contacts. We prepared three different vertical double QD devices (devices A, B, and C) to study J vs Δ, as well as the influence of interdot tunnel coupling t. Devices A and B have almost the same t but different tunable ranges of Δ with V_{sd}. Using devices A and B, we can cover the whole range of Δ between $\Delta = 0$ and $\Delta = \Delta_T$. Device C has a smaller t than devices A and B. We use this device to discuss the influence of t on J.

Figure 1(a) shows a schematic diagram of the devices. All the devices have almost the same geometry, consisting of a gated submicron pillar with a triple barrier structure (TBS). The TBS for devices A and B is composed of two 7.0-nm-thick $Al_{0.3}Ga_{0.7}As$ outer barriers, an $Al_{0.3}Ga_{0.7}As$ center barrier of 6.0-nm (device A) and 6.5-nm (device B) thickness and two 10.0-nm-thick GaAs wells. For device C, the TBS consists of three 8.0-nm $Al_{0.22}Ga_{0.78}As$ barriers and two 12.0-nm $In_{0.05}Ga_{0.95}As$ wells [14,15]. The two QDs are vertically coupled through the center barrier and laterally confined by a Ti/Au Schottky gate surrounding the pillar. For all the devices, the number N of electrons in the double QD can be reduced down to $N = 0$ more or less in a similar manner as the gate voltage is made more negative.

The energy diagram for the two-electron states in the double QD is shown in Fig. 1(b), with the energy detuning Δ between the two QDs, QD1 and 2, as a parameter. Two singlet states, $S(0, 1s1s)$ having two electrons in the same lowest orbital state or $1s$ state of QD1 and $S(1s, 1s)$ having two electrons in the $1s$ state of the two QDs, are in resonance at $\Delta = 0$, while two triplet states $T(1s, 1s)$ having two electrons in the $1s$ states of the two QDs and $T(0, 1s2p)$ having two electrons in the two lowest orbital states, i.e., $1s$ and $2p$ state of QD1, are in resonance at $\Delta = \Delta_T$ [16]. Once $T(1s, 1s)$ is occupied in the PSB region, further electron transfer is prohibited by Pauli exclusion, unless a transition from $T(1s, 1s)$ via $S(1s, 1s)$ to $S(0, 1s1s)$ occurs. The PSB is lifted either by $T(1s, 1s) - T(0, 1s2p)$ resonance or when the energy of a one-electron state $(0, 1s)$ having one electron in the $1s$ state of QD1 becomes higher than the Fermi energy of the drain contact.

Figure 1(c) shows the differential conductance dI_{sd}/dV_{sd} versus V_{sd} and gate voltage V_g measured for device A at 1.5 K. The total electron number N in the double QD is indicated for the two Coulomb blockade (CB) regions bounded by the dotted line with the center at $V_{sd} = 0$. To the right of the $N = 2$ CB, there is a region of suppressed dI_{sd}/dV_{sd} due to PSB. The energy diagrams of PSB and S-S resonance are indicated. S-S resonance is assumed to occur at $V_{sd} = 0$ from the fact that the upper boundary of the $N = 1$ CB diamond closes [17]. PSB is observed in the V_{sd} range near S-S resonance in this device. In the PSB region, a finite small leakage current ($\sim$ few hundred fA) flows, mainly due to second-order cotunneling [18] as well as tunneling with spin flip induced by the hyperfine interaction and the spin-orbit interaction. Here, we focus on the leakage current due to the hyperfine interaction because it shows a clear hysteresis for sweeping up and down the magnetic field as a good signature of DNP [6,12]. To assure a contribution from the hyperfine interaction, we performed NMR experiments in the PSB region. Figure 1(d) shows the frequency dependence of the leakage current in the presence of a static in-plane magnetic field of $B_{in} = 300$ mT. The NMR signals were observed at 2.15 MHz, 3.05 MHz, and 3.85 MHz. Figure 1(e) shows the B_{in} dependence of the NMR frequency. From the linear dependence with B_{in} we obtain proportional constants of 7.17 ± 0.17 MHz/T, 10.07 ± 0.04 MHz/T, and 12.84 ± 0.03 MHz/T for the NMR signals, which are consistent with those of ^{75}As (7.292 MHz/T), ^{69}Ga (10.219 MHz/T), and ^{71}Ga (12.984 MHz/T), respectively, in the literature [19]. Note that in our previous NMR measurements using $In_{0.05}Ga_{0.95}As$ double QDs instead of GaAs double QDs, we observed no ^{75}As resonance. This difference is probably due to the influence of In atoms [20]. A random distribution of In atoms in the InGaAs well causes an inhomogeneous strain in the host material of the QDs, which can cause large broadening of the NMR peaks in the InGaAs QDs.

Figure 2(a) shows the magnetic field B_{in} dependence of the leakage current I_{sd} measured at $V_{sd} = 0.8$ to 2 mV in the PSB region. B_{in} was swept from 0 T up to 0.3 T and then down to 0 T with a sweep rate of 1 T/h. For all of the data curves, I_{sd} is constant as B_{in} initially increases, then increases with a sharp step (indicated by arrows) at $B_{in} = B_{sw}$, and finally becomes saturated for B_{in} up to 0.3 T. As B_{in} decreases from 0.3 T, I_{sd} gradually decreases to the initial current level. This behavior is schematically shown in Fig. 2(b) and assigned to a S-T transition mediated by the hyperfine interaction. The magnetic field lifts the $T(1s, 1s)$ degeneracy into three substates, T_+, T_0, and T_- with S_z components of 1, 0, and -1, respectively. The T_- and $S(1s, 1s)$ state becomes degenerate at $B_{in} = B_{sw}$, as shown in Fig. 2(c). The transition between these two states is then promoted by a hyperfine mediated spin flip-flop transition, conserving energy. This progressively occurs as B_{in} approaches B_{sw}, because the T_- to S transition accompanies DNP to pump the down nuclear spins, and therefore give a positive feedback to B_{in} [5]. PSB is partially but

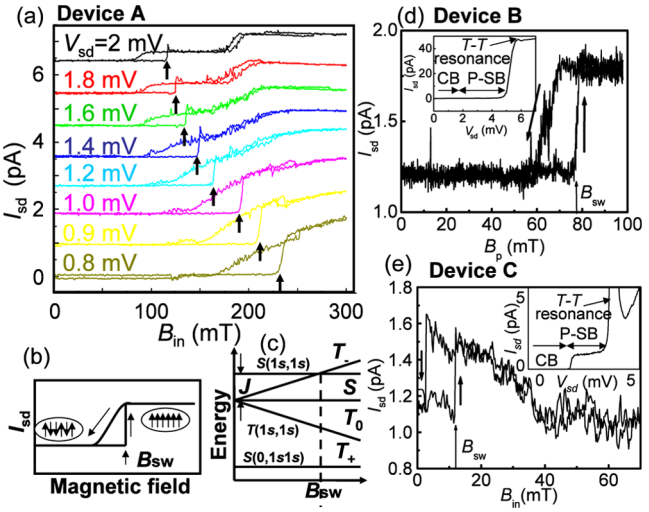

FIG. 2 (color online). (a) In-plane magnetic field (B_{in}) dependence of the leakage current I_{sd} measured at $I_{sd} = 0.8$ mV to 2 mV in the PSB region. Each curve is offset upwards by 1 pA. (b) Schematic hysteretic behavior in the $I_{sd} - B$ plane. The nuclear spins in the QDs polarize above $B = B_{sw}$. (c) Zeeman effect on the S and T states. The S state and T_- states become degenerate at B_{sw}. (d) I_{sd} as a function of B_p measured at $V_{sd} = 2.5$ mV in the PSB region. The sweep rate is 1 T/hour. Inset to (d): I_{sd} vs V_{sd} measured at $T = 30$ mK, showing the PSB for $1.2\ \text{mV} < V_{sd} < 5$ mV. The peak at $V_{sd} \sim 6.8$ mV is due to $T(1s, 1s) - T(0, 1s2p)$ resonance. (e) B_{in} dependence of I_{sd} measured at $V_{sd} = 3$ mV in the PSB region. Inset to (e): I_{sd} vs V_{sd} showing PSB for $2\ \text{mV} < V_{sd} < 3.5$ mV. The peak at $V_{sd} = 3.8$ mV is due to $T(1s, 1s) - T(0, 1s2p)$ resonance.

abruptly lifted when $B_{in} \sim B_{sw}$, so the leakage current increases with a step. Therefore, the threshold magnetic field B_{sw} is assumed to be a measure of J as given by $E_Z = g\mu_B B_{sw} = J$. In Fig. 2(a) we find that as the set V_{sd} decreases, B_{sw} or J increases more abruptly for V_{sd} near the S-S resonance. We observe a two-step increase of the leakage current and a slight decrease following the jump-up at the first step in the top four curves for $V_{sd} > 1.2$ mV. This may be due to the difference of the nuclear spin state between the two QDs and the related relaxation process, although the underlying physics is not clear.

In device B, PSB is observed in the V_{sd} range from 1.5 to 5 mV, and lifts for $V_{sd} > 5$ mV, bounded by $T(1s, 1s) - T(0, 1s2p)$ resonance, as shown in the inset to Fig. 2(d). We fixed V_{sd} at $V_{sd} = 2.5$ mV in the PSB region and measured I_{sd} as a function of the perpendicular magnetic field B_p. Note that the applied B_p field is so small (<120 mT) that the influence on the orbital states can be neglected. We again observe a steplike increase of the leakage current on sweeping up the magnetic field. We use device C to evaluate J near the T-T resonance but away from the S-S resonance. We initially fixed the gate voltage such that I_{sd} vs V_{sd} shows a CB region for $V_{sd} < 2$ mV, T-T resonance at $V_{sd} \sim 3.8$ mV, and a PSB region in between [inset to Fig. 2(e)]. We then measured the leakage current in the middle of the PSB region as a function of B_{in}, as shown in Fig. 2(e).

The B_{sw} fields evaluated from the measured $I_{sd} - B$ hysteretic loops are plotted as a function of Δ/Δ_T in Fig. 3. The squares and circles indicate the B_{sw} values obtained for devices A and B, respectively. For device A, as Δ/Δ_T increases from 0.13 to 0.4, B_{sw} decreases, reflecting the decrease of J. For device B, as Δ/Δ_T increases, B_{sw} gradually decreases for Δ/Δ_T from 0.42 to 0.5, remains almost constant for Δ/Δ_T to 0.8, and gradually increases for Δ/Δ_T to 0.9. Here we use the relation $J = |g|\mu_B B_{sw}$ with $|g| = 0.23$ [21–23] to make an ordinate for J in Fig. 3 to the right. J ranges from 1.3 to 3.5 μeV for device A and from 0.9 to 1.3 μeV for device B. The increase of B_{sw} with Δ/Δ_T approaching $\Delta/\Delta_T = 0$ for device A and $\Delta/\Delta_T = 1$ for device B compares to J enhanced by S-S, and T-T resonance, respectively.

In the inset to Fig. 3 we show B_{sw} observed for device C (triangle), which gradually increases as V_{sd} increases from 2.5 to 3.5 mV. In order to calibrate J with B_{sw}, we use $|g| = 0.30$, previously derived for InGaAs vertical double QDs [24]. J ranges from 0.15 to 0.3 μeV, shown by the triangles in the main panel of Fig. 3 for comparison, and is almost 1 order of magnitude smaller than that for devices A and B, reflecting the small t for device C. We use the Hubbard model including the $1s$ and $2p$ states in QD1 and the $1s$ state in QD2 to calculate the exchange energy J. The $2p$ state in QD2 is neglected because it is located at a very high energy. For the T states, the diagonal energies of the Hamiltonian matrix elements are $E_{T(1s,1s)} = V + \delta$ and $E_{T(0,1s2p)} = U + \hbar\omega - U_{ex} - xeV_{sd}$, using only the basis of $T(1s, 1s)$ and $T(0, 1s2p)$. Here, U and V are the intra- and interdot Coulomb energies, $\hbar\omega$ and U_{ex} are confinement energy and exchange energy in QD1, δ is the energy difference between QD1 and 2 at $V_{sd} = 0$, and x is the conversion factor of the increment between V_{sd} and Δ. The off-diagonal energy is $\sqrt{2}t_T$, where t_T is the tunnel coupling between the $T(1s, 1s)$ and $T(0, 1s2p)$ states. We define $U' \equiv U + \hbar\omega - U_{ex}$ for simplicity. Thus, the

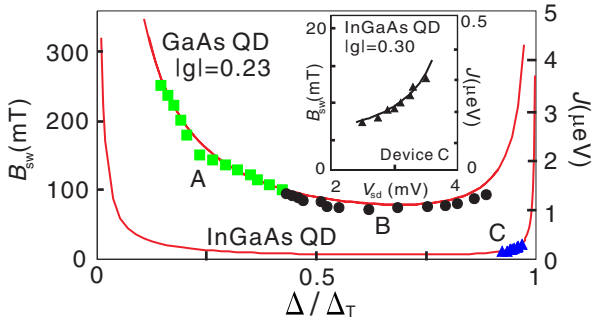

FIG. 3 (color online). B_{sw} plotted as a function of Δ/Δ_T. Right-hand side scale: Exchange energy J of devices A (square), B (circle), and C (triangle) derived experimentally and theoretically (solid line) as a function of Δ/Δ_T. Inset: Magnification of B_{sw} and J for device C as a function of V_{sd}.

eigenenergies are derived as

$$E_{T(T^*)} = \tfrac{1}{2}(V + \delta + U' - xeV_{\mathrm{sd}} - (+)\sqrt{(V + \delta - U' + xeV_{\mathrm{sd}})^2 + 8t_T^2}). \quad (1)$$

Similarly for the S states, the diagonal energies of the Hamiltonian matrix elements are $E_{S(1s,1s)} = V + \delta$ and $E_{S(0,1s1s)} = U - xeV_{\mathrm{sd}}$, respectively, and the off-diagonal energy is $\sqrt{2}t_S$, where t_S is the tunnel coupling between the $S(1s, 1s)$ and $S(0, 1s1s)$ states. The eigenenergies are given by

$$E_{S(S^*)} = \tfrac{1}{2}(V + \delta + U - xeV_{\mathrm{sd}} - (+)\sqrt{(V + \delta - U + xeV_{\mathrm{sd}})^2 + 8t_S^2}). \quad (2)$$

Then, J is derived as

$$J = E_{S^*} - E_T = \tfrac{1}{2}(\sqrt{\Delta^2 + 8t_S^2} - \sqrt{(\Delta_T - \Delta)^2 + 8t_T^2} - \Delta_T). \quad (3)$$

Here, we use the equations $\Delta_T = \hbar\omega - U_{\mathrm{ex}}$ and $\Delta = xeV_{\mathrm{sd}} + U - V - \delta = xeV_{\mathrm{sd}} + \Delta_{\mathrm{sd}}$. In order to calculate J for devices A and B, we used the values $\Delta_{\mathrm{sd}} = 0.11$ meV for device A and 0.2 meV for device B, and $\Delta_T = 1.86$ meV for both devices, all derived by analyzing the Coulomb diamond data. We calculate the J values with t_S and t_T as fitting parameters to reproduce the experiment. The result is shown by the solid line in Fig. 3. The experimental data are nearly perfectly reproduced by the calculations using $t_S = 22$ μeV and $t_T = 10$ μeV for both devices. The ratio of t_S and t_T is reasonable when ''incoherent tunneling'' is considered [25]. The calculated ratio of the incoherent tunneling between the $1s$ state in the two QDs and that between the $1s$ state in one QD and the $2p$ state in the other QD is 2:1. Based on this, we used $\Delta_{\mathrm{sd}} = 2.1$ meV and $\Delta_T = 5.66$ meV to calculate J for device C. The experimental data are also well reproduced by the calculations for device C using $t_S = 11$ μeV and $t_T = 5$ μeV. These t_S and t_T values are smaller than those for devices A and B, as expected.

In conclusion, we use the lifting of PSB by hyperfine coupling to nuclear spins to quantitatively evaluate the exchange energy J over a wide range of interdot level detuning Δ using three kinds of vertical double QDs. J is enhanced near the S-S and T-T resonance points, reflecting the hybridization of the two resonant states. The obtained data of J are fully reproduced over the whole Δ range by Hubbard model calculations. We also show the contribution from all ^{69}Ga, ^{71}Ga, and ^{75}As nuclear spins to the PSB lifting using an NMR technique.

The authors thank M. Stopa for fruitful discussions. This work was financially supported by Grants-in-Aid for Scientific Research S (No. 19104007), B (No. 18340081), and by ERATO-JST and Special Coordination Funds for Promoting Science and Technology. S. T. acknowledges support from QuEST program (BAA-0824).

*kodera@iis.u-tokyo.ac.jp

[1] D. Loss and D. P. DiVincenzo, Phys. Rev. A **57**, 120 (1998).
[2] M. A. Nielsen and I. L. Chuang, *Quantum Computation and Quantum Information* (Cambridge University Press, New York, 2000).
[3] T. Hatano *et al.*, Science **309**, 268 (2005).
[4] W. G. van der Wiel *et al.*, Rev. Mod. Phys. **75**, 1 (2002).
[5] J. Baugh *et al.*, Phys. Rev. Lett. **99**, 096804 (2007).
[6] K. Ono and S. Tarucha, Phys. Rev. Lett. **92**, 256803 (2004).
[7] A. C. Johnson *et al.*, Nature (London) **435**, 925 (2005).
[8] J. R. Petta *et al.*, Science **309**, 2180 (2005).
[9] F. H. L. Koppens *et al.*, Nature (London) **442**, 766 (2006).
[10] F. H. L. Koppens *et al.*, Science **309**, 1346 (2005).
[11] E. A. Laird *et al.*, Phys. Rev. Lett. **97**, 056801 (2006).
[12] S. Tarucha *et al.*, Phys. Status Solidi B **243**, 3673 (2006).
[13] T. Kodera *et al.*, Physica (Amsterdam) **40E**, 1139 (2008).
[14] T. Kodera *et al.*, Physica (Amsterdam) **22E**, 518 (2004).
[15] D. G. Austing *et al.*, Jpn. J. Appl. Phys. **36**, 1667 (1997).
[16] V. Fock, Z. Phys. **47**, 446 (1928).
[17] K. Ono *et al.*, Science **297**, 1313 (2002).
[18] I. Weymann, Phys. Rev. B **78**, 045310 (2008).
[19] C. P. Slichter, *Principles of Magnetic Resonance* (Springer-Verlag, Berlin, 1990), 3rd ed.
[20] C. Deng and X. Hu, Phys. Rev. B **71**, 033307 (2005).
[21] T. Kodera *et al.*, in *Proceedings of the International Symposium on Mesoscopic Superconductivity and Spintronics 2004* (World Scientific, Singapore, 2005), p. 445.
[22] M. J. Snelling *et al.*, Phys. Rev. B **44**, 11345 (1991).
[23] R. Hanson *et al.*, Phys. Rev. Lett. **91**, 196802 (2003).
[24] Y. Nishi *et al.*, Phys. Rev. B **74**, 033306 (2006).
[25] K. Ono *et al.*, Physica (Amsterdam) **314B**, 450 (2002).